THE JOURNAL OF BIOLOGICAL CHEMISTRY VOL. 285, NO. 3, pp. 2003–2013, January 15, 2010

Crystal Structure of the Protealysin Precursor

*INSIGHTS INTO PROPEPTIDE FUNCTION**

Received for publication, May 29, 2009, and in revised form, November 11, 2009 Published, JBC Papers in Press, November 13, 2009, DOI 10.1074/jbc.M109.015396

Ilya V. Demidyuk[‡1], Tania Yu. Gromova[‡], Konstantin M. Polyakov[§], William R. Melik-Adamyan[¶], Inna P. Kuranova[¶], and Sergey V. Kostrov[‡]

From the [‡]Institute of Molecular Genetics, Russian Academy of Sciences, Kurchatov Sq. 2, Moscow 123182, Russia, the [§]Kurchatov Center for Synchrotron Radiation and Nanotechnology, Kurchatov Sq. 1, Moscow 123182, Russia, and the [¶]Shubnikov Institute of Crystallography, Russian Academy of Sciences, Leninsky Av. 59, Moscow 119333, Russia

Protealysin (PLN) belongs to the M4 family of peptidases that are commonly known as thermolysin-like proteases (TLPs). All TLPs are synthesized as precursors containing N-terminal propeptides. According to the primary structure of the N-terminal propeptides, the family is divided into two distinct groups. Representatives of the first group including thermolysin and all TLPs with known three-dimensional structures have long prosequences (~200 amino acids). Enzymes of the second group, whose prototype is protealysin, have short (~50 amino acids) propeptides. Here, we present the 1.8 Å crystal structure of PLN precursor (proPLN), which is the first three-dimensional structure of a TLP precursor. Whereas the structure of the catalytic domain of proPLN is similar overall to previously reported structures of mature TLPs, it has specific features, including the absence of calcium-binding sites, and different structures of the N-terminal region and substrate-binding site. PLN propeptide forms a separate domain in the precursor and likely acts as an inhibitor that blocks the substrate-binding site and fixes the "open" conformation of the active site, which is unfavorable for catalysis. Furthermore the conserved PPL motif identified in our previous studies directly interacts with the S′ subsites of the active center being a critical element of the propeptide-catalytic domain interface. Comparison of the primary structures of TLPs with short propeptides suggests that the specific features revealed in the proPLN crystal structure are typical for all protealysin-like enzymes. Thus, such proteins can be considered as a separate subfamily of TLPs.

Thermolysin-like proteases (TLPs)[2], or peptidases of the M4 family (1), are one of the best known groups of proteolytic enzymes. TLPs are found in dozens of Gram-positive and -negative bacterial species as well as in fungi and the archaeon *Methanosarcina acetivorans* (for reference see MEROPS database; 2). Many TLPs are produced by pathogenic organisms and thus can serve as potential drug targets; in addition, they have a considerable innovative potential for biotechnological application (see Ref. 3 for review). The family prototype thermolysin (MEROPS database identifier M04.001) was one of the first metallopeptidases to be sequenced (4) and one of the first to have its tertiary structure determined (5). To date, dozens of crystal structures of thermolysin with various ligands as well as crystal structures of TLPs from *Bacillus cereus* (6, 7), *Pseudomonas aeruginosa* (8), and *Staphylococcus aureus* (9) have been reported. Similar to many other proteolytic enzymes, TLPs are synthesized as precursors carrying N-terminal propeptides also called proregions or prosequences. No three-dimensional structures of TLP precursors are currently available.

According to the primary structure of their propeptides, peptidases of the M4 family are divided into two distinct groups, although the mature enzymes have largely similar sequences (10). Propeptides of the first group of proteins are similar to that of thermolysin (TLN) and are ~200 amino acids long (long propeptides). Such propeptides are found in all enzymes with determined three-dimensional structures of the mature portion. Thermolysin type propeptides are known to be crucial for enzyme functioning. They act as intramolecular chaperones (11–14), can inhibit cognate mature proteins (14–17), and influence their secretion (12, 18). Proteins of the second group resemble protealysin from *Serratia proteamaculans* (MEROPS ID M04.025) (19) by the structure of their ~50-amino acid propeptide. This group includes about one-fourth of TLPs; however, the functions of protealysin-like propeptides remain unclear.

The situation with TLP propeptides is intriguing. Their structures substantially differ at the background of highly similar catalytic domains. Moreover, the same species can produce enzymes with both propeptide types (10). This may indicate that the propeptides rather than the catalytic domains determine the biological function of M4 peptidases. If so, TLP propeptides can be considered as original evolutionary modules adapting the catalytic domains of proteases to cell requirements. However, the available structural and biochemical data are insufficient to understand how this system functions.

In this paper, we report the crystal structure of protealysin precursor, which is the first crystal structure of a precursor of thermolysin-like proteases as well as the first crystal structure of an enzyme from protealysin subfamily of M4 peptidases. The

* This work was supported in part by the Russian Foundation for Basic Research (Projects 09-04-00734 and 09-04-00870), the Program for Molecular and Cell Biology of the Russian Academy of Sciences, and the Federal Program "R&D in Priority Directions of the Russian Scientific-Technological Complex Development in 2007–2012" (State Contract 02.512.12.2050).

The atomic coordinates and structure factors (code 2VQX) have been deposited in the Protein Data Bank, Research Collaboratory for Structural Bioinformatics, Rutgers University, New Brunswick, NJ (http://www.rcsb.org/).

[1] To whom correspondence should be addressed: Kurchatov Sq. 2, Moscow 123182, Russia. Tel.: 7-499-196-1853; Fax: 7-499-196-0221; E-mail: duk@img.ras.ru.

[2] The abbreviations used are: TLP, thermolysin-like protease; TLN, thermolysin; PAE, *P. aeruginosa* elastase; PLN, protealysin; proPLN, protealysin precursor; PDB, Protein Data Bank.

data obtained give us an insight to the functioning of TLP propeptides and the underlying mechanism as well as demonstrate the difference between the catalytic domains of the two groups of the family.

EXPERIMENTAL PROCEDURES

Mutant Protein Construction, Expression, and Purification—ProPLN with a substitution of the key active site residue Glu-163 to Ala (numbering starts from the initial Met of PLN; Glu-163 corresponds to Glu-143 in mature TLN) and carrying a His_6 tag at the C terminus was constructed, overproduced in *Escherichia coli*, and purified as described previously (20, 21). After purification, proPLN solution was dialyzed against 10 mM ammonium acetate and lyophilized.

The N-terminal amino acid sequence was determined after proPLN transfer onto a polyvinylidene difluoride membrane (Amersham Biosciences) using Edman auto-degradation on a 477A protein/peptide sequencer equipped with a 120A PTH amino acid analyzer (Applied Biosystems). The mass spectrometric analysis of proPLN was performed on a high resolution electrospray ionization orthogonal injection time-of-flight mass spectrometer (22).

Crystallization, Data Collection, and Structure Determination—The mutant proPLN was crystallized at room temperature as described previously (20) by the hanging-drop vapor diffusion method against a precipitant solution of 15% polyethylene glycol monomethyl ether 2000, 0.2 M ammonium sulfate, and 0.1 M sodium acetate, pH 4.6. Droplets contained 3 μl of 10 mg/ml protein solution and 1.5 μl precipitant solution with 0.06% octyl β-D-glucopyranoside in the same buffer. Crystals grew to maximum dimensions of 0.5 × 0.3 × 0.05 mm. Before data collection, the crystals were cryoprotected by rapid soaking in a solution containing mother liquor supplemented with 10% (v/v) glycerol and flash cooled with a nitrogen cryostream. X-ray diffraction data were collected on the K4.4 beamline of the Kurchatov Center for Synchrotron Radiation and Nanotechnology (Moscow, Russia) using a MAR CCD detector (23). For structure determination, a diffraction data set to 1.8 Å resolution was collected at a wavelength of 0.99 Å at 100 K. The diffraction images were processed and scaled with the XDS package (24). The proPLN crystals belonged to the space group $P2_12_12$, with cell dimensions of $a = 70.76$, $b = 78.65$, and $c = 59.28$ Å and $\alpha, \beta, \gamma = 90.0°$. There was one protein molecule per asymmetric unit. Structure determination was carried out with the BALBES (25) and MOLREP (26) programs using the structure of neutral protease from *B. cereus* (Protein Data Bank (PDB) accession code 1NPC) as the starting model. The starting model was modified and refined by using the CCP4 program suite for protein crystallography (27) and the REFMAC program (28) and manually processed with the COOT graphics program (29). An electron density map corresponding to the proPLN structure was calculated after refinement by REFMAC using coefficients ($2mF_o - DF_c$) (30). An omit map was calculated after refinement of the model lacking the propeptide residues using coefficients ($mF_o - DF_c$) (30). The final structure contained amino acid residues 6–37 and 52–341, one Zn^{2+} ion, and 277 water molecules yielding a crystallographic *R* factor of 17.1% and a free *R* factor of 20.2%. Seven residues (Cys-29, Glu-67, Asp-102, Met-229, Asn-260, Asp-305, and Ser-325) were modeled with alternate conformations. The details of data collection, processing, and structure refinement are summarized in Table 1. The coordinates and structure factors have

TABLE 1
Data collection and structural refinement statistics

Data collection statistics	
Space group	$P2_12_12$ (No. 18)
Cell parameters	$a = 70.76$, $b = 78.65$, $c = 59.28$ Å; $\alpha = \beta = \gamma = 90°$
Resolution range (Å)	52.6–1.8 (2.0–1.8)[a]
No. unique reflections	28551 (6565)
Completeness (%)	90.9 (78.6)
B factor from Wilson plot (Å^2)	22.9
Average $I/\sigma(I)$	26.92 (11.07)
Multiplicity	2.82 (2.66)
R_{meas} (%)[b]	3.2 (10.7)
$R_{mrgd\text{-}F}$ (%)[b]	4.2 (12.5)
Model refinement statistics	
Resolution (Å)	52.6-1.82
No. of reflections	27076
R_{cryst} (%)[c]	17.1
R_{free} (%)[d]	20.2
No. non-hydrogen atoms	2805
No. water molecules	277
B factors (Å^2)	
Averaged	15.07
Main chain	13.62
Side chains	14.80
Water molecules	23.07
Estimated coordinate error (Å)[e]	0.14
RMS[f] deviations from ideality	
Bond lengths (Å)	0.01
Bond angles	1.04°
Model geometry[g]	
Rotamer outliers	0.78
Ramachandran outliers	0.00
Ramachandran favored	97.2

[a] Values in parentheses correspond to the highest resolution shell.
[b] For definition of R_{meas} and $R_{mrgd\text{-}F}$, see Ref. 51.
[c] $R_{cryst} = \Sigma||F_{obs}| - |F_{calc}||/\Sigma|F_{obs}|$.
[d] R_{free} is as for R_{cryst} but calculated for a test set comprising 5% reflections not used in the refinement.
[e] Based on maximum likelihood.
[f] RMS, root mean square.
[g] Analyze was performed using MOLPROBITY (52).

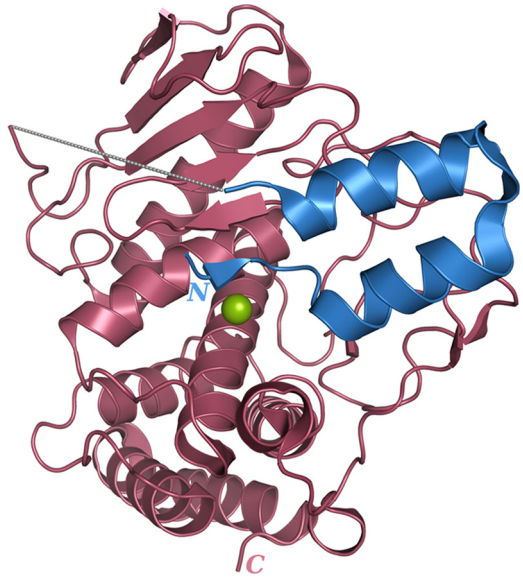

FIGURE 1. **Overview of the protealysin precursor structure.** The catalytic domain and propeptide are shown in *brown* and *blue*, respectively. The 38–51 region of protealysin precursor is indicated by a *gray dashed line*. The catalytic zinc ion is represented by a *green sphere*.

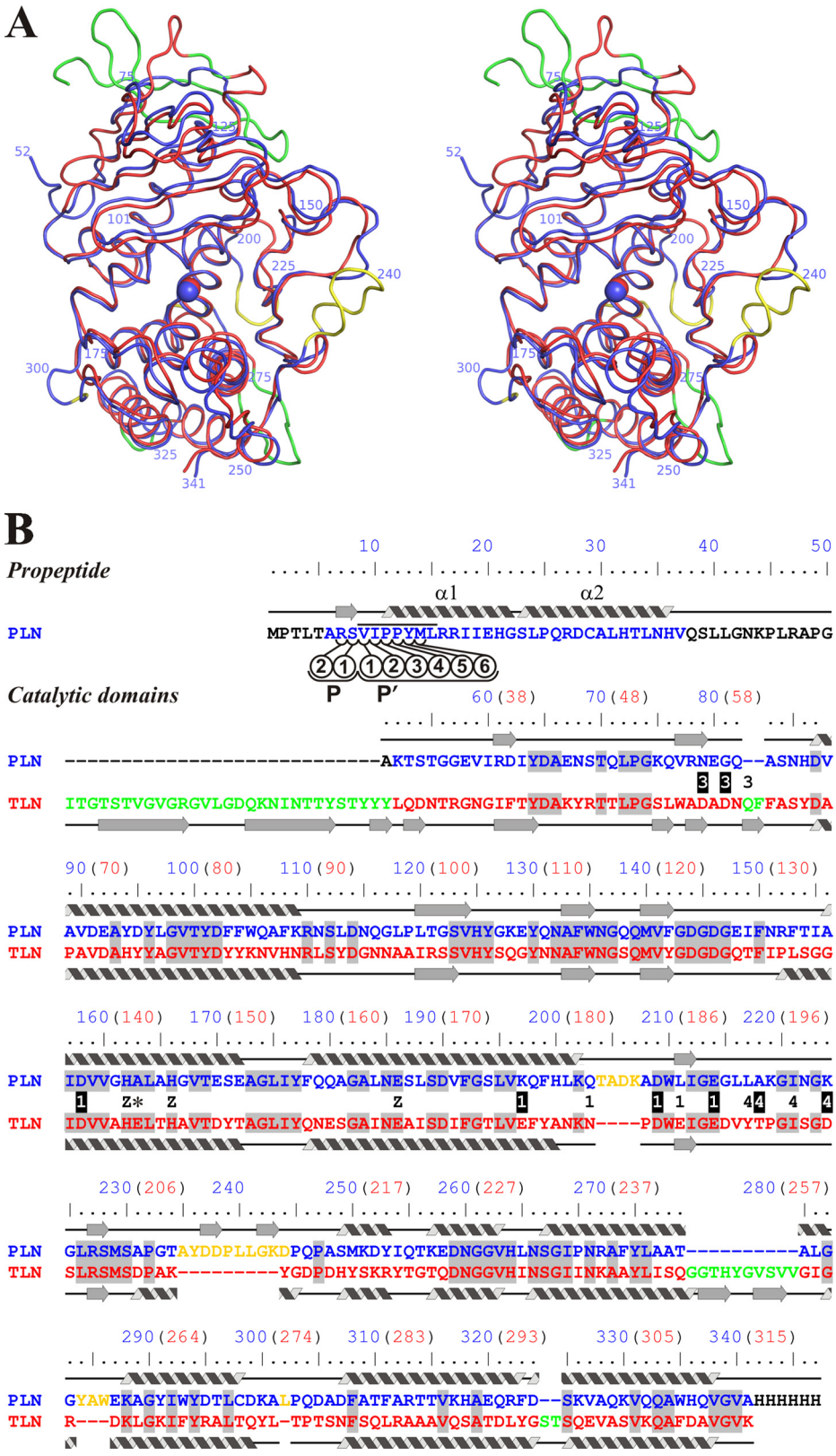

FIGURE 2. **Comparison of three-dimensional structures of protealysin (PLN, *blue*) and thermolysin (PDB code 8TLN; TLN, *red*).** *A*, stereoview of superposition of Cα backbones of PLN and TLN (root mean square = 1.06 Å). *B*, three-dimensional structure-based sequence alignment. Secondary structures of PLN and TLN are presented over and under sequences, respectably. Numbering corresponds to proPLN (numbers in *blue*); for reference, numbering corresponding to mature TLN is given in *parentheses* (numbers in *red*). PLN *versus* TLN insertions are shown in *yellow*; TLN *versus* PLN insertions are shown in *green*. Residues that are Ca^{2+} ligands in TLN are marked with numbers: *1*, Ca1/2; *3*, Ca3; and *4*, Ca4. Ligands whose side chains interact with Ca^{2+} are marked by *white numbers* on a *black background*. *Z* indicates zinc ion ligands; an *asterisk* indicates the Glu-163→Ala modification site. The residues undetectable in the electron density maps are shown in *black*. Amino acids identical in PLN and TLN are *shaded*. The PPL motif is *overlined*. The propeptide residues interacting with the substrate-binding site are designated as P1, P2, P1′, P2′, P3′, P4′, P5′, and P6′ according to Schechter and Berger (40).

been deposited in the Protein Data Bank under accession code 2VQX.

Structure and Sequence Analysis—Multiple sequence alignments were constructed by ClustalX 1.8 using the Gonnet series of protein weight matrices (31). The set of TLP sequences described previously (10) was used for alignment. The sequence logo (32) was generated using the WebLogo tool (33). Structure superimpositions were performed using DeepView (34) or PyMOL (35). All three-dimensional structure figures were generated using PyMOL.

RESULTS AND DISCUSSION

Overall Structure—Similar to all M4 peptidases, protealysin (PLN) is synthesized as a precursor with an N-terminal propeptide. The native protealysin precursor (proPLN) is unstable and autocatalytically processed in solution to mature active protein (21). The introduced Glu-163→Ala mutation (hereafter, numbering starts from the initial Met of PLN) prevented proPLN maturation, which allowed the isolation of preparative quantities of the full-length precursor. The protein was crystallized, and its three-dimensional structure was determined using x-ray crystallography, which yielded the first crystal structure of an M4 peptidase precursor.

The propeptide forms a separate domain in the proPLN molecule (Fig. 1) and interacts with the catalytic portion in the active center region. The N-terminal region of the propeptide occupies the substrate-binding site of the enzyme. It should be noted that we failed to identify some parts of the proPLN molecule in the electron density maps: 2–5, 38–51, and 342–347. At the same time, the molecular mass determined by mass spectrometry (38,103 Da) and the N-terminal sequence (PTLTAR) of the purified protein used in crystallization correspond to the entire precursor without the start methionine, with the Glu-163 to Ala substitution in the active site, and with a His_6 tag at the C terminus. These findings sug-

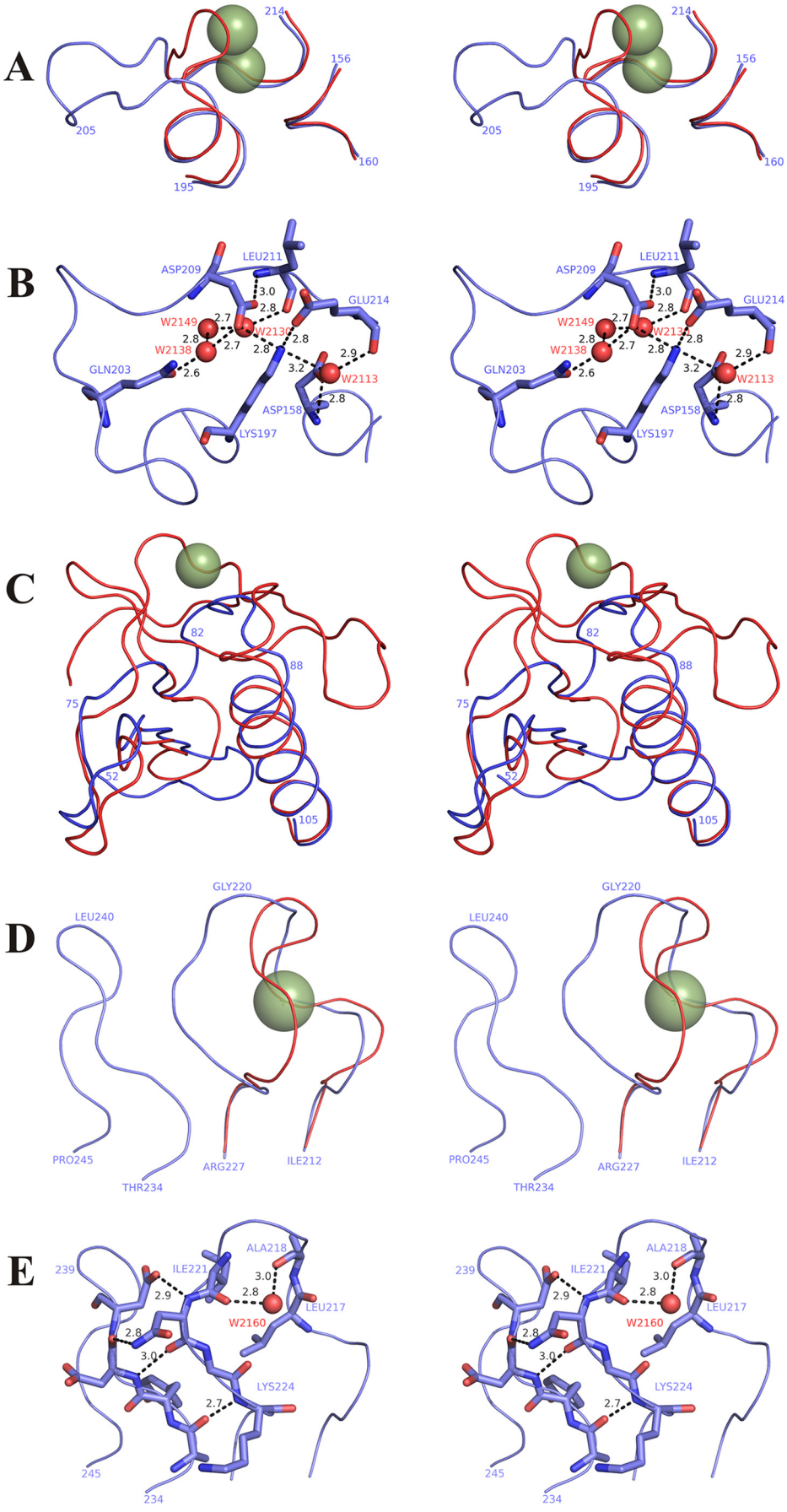

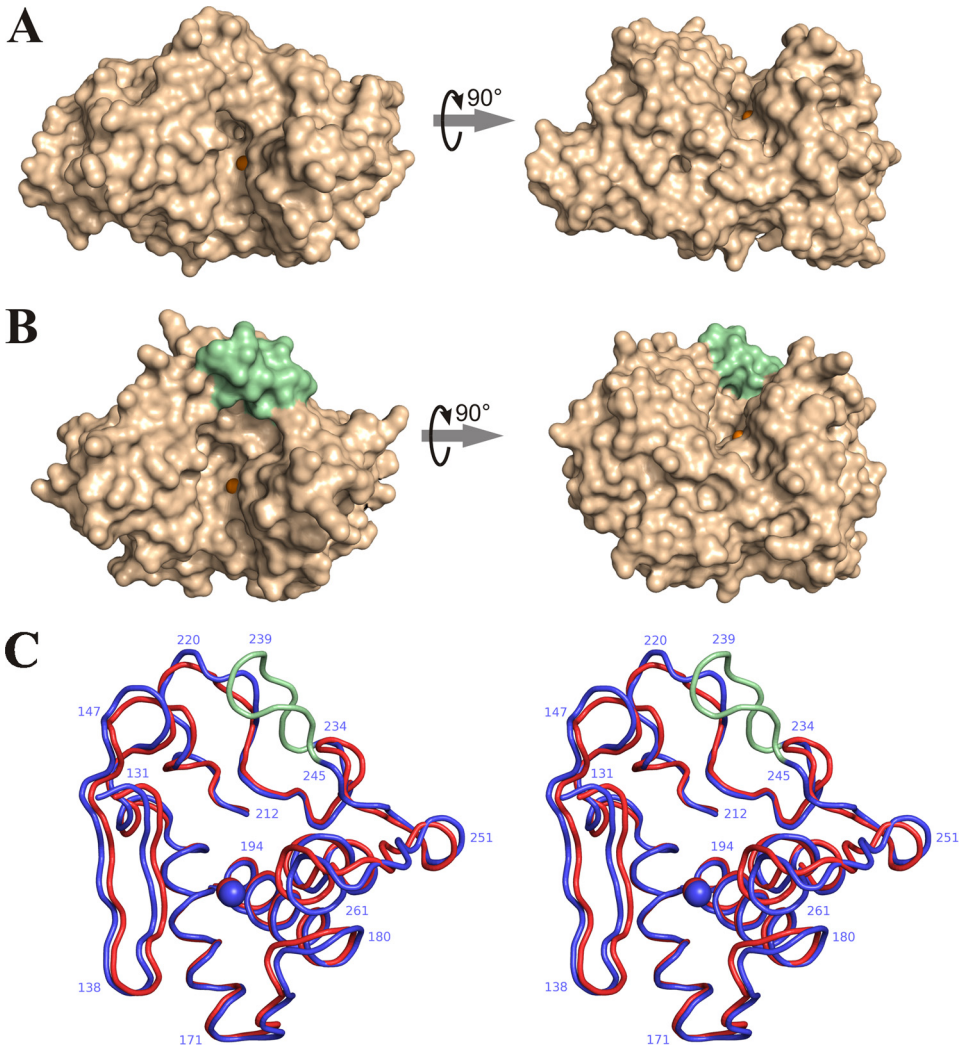

FIGURE 4. **Comparison of active site geometry in thermolysin (PDB code 8TLN) and protealysin.** *A*, surface view of TLN; *B*, surface view of PLN; *C*, stereoview of superposition of the Cα backbone in the active site region of TLN (*red*) and PLN (*blue*). The AYDD-hairpin is shown in *pale green*; the catalytic zinc ions are shown as *orange spheres*; *numbering* corresponds to proPLN sequence.

gest high flexibility of these parts, which can be attributed to the N- and C-terminal position of the 2–5 and 342–347 (the His_6 tag) regions, respectively. The flexibility of the 38–51 region can be of functional significance. This region including 13 C-terminal amino acids of the propeptide and the first residue of the mature domain contains cleavage sites of autocatalytic removal of the propeptide, and the heterocatalytic processing of proPLN likely occurs here too (21). Thus, the 38–51 flexible loop exposed for a wide range of endopeptidases likely provides for efficient removal of the PLN propeptide.

Catalytic Domain Structure—The three-dimensional structure of the PLN mature domain is largely similar to that of TLN (Fig. 2) and other TLPs (data not shown); however, there are several highly significant local differences.

We failed to detect calcium ions in the PLN structure, although all M4 peptidases with known three-dimensional structures bind one to four ions of this metal (5–9). Note that the significance of calcium binding for protein stabilization was demonstrated in all cases studied; accordingly, the thermostability increased with Ca^{2+} concentration (36–39). Analysis of the PLN structure in the regions corresponding to calcium binding sites in TLN and other TLPs demonstrated their notable difference in PLN.

The most surprising differences were observed in the region corresponding to the main double calcium-binding site in TLN (Ca1/2) (Fig. 3, *A* and *B*). Although most calcium ligands exist in PLN (Figs. 2*B* and 3*B*), the $Glu\text{-}177_{TLN}$ to Lys-197 substitution (the subscript name indicates the protein whose residue is concerned except PLN whose name is omitted; TLN numbering corresponds to the mature protein) introduces an ionic interaction and additional hydrogen bonds in the PLN molecule (Fig. 3*B*). These interactions, as though compensating for missing coordination bonds with calcium ions, directly involve (apart from Lys-197) Asp-209 and Glu-214, analogs of the main Ca^{2+} ligands in TLN. Note that Asp-158 (an analog of another calcium ligand interacting by a side chain) is not involved in the above-mentioned interaction. The carboxyl group of Asp-158 forms hydrogen bonds with the amide group of Gly-213 and water molecule HOH-2113. The ^{204}TADK^{207} and ^{284}YAW^{286} insertions are other significant differences between this region in PLN and Ca1/2 in TLN. These insertions give rise to another set of interactions stabilizing the structure of this region, primarily, the Gly-285 O–Ala-205 N hydrogen bond and hydrophobic contacts of Tyr-284 and Trp-286 side chains with the aromatic rings of Phe-199 and Phe-103. Amino acid sequence comparison of the enzymes with short propeptides (data not shown) demonstrates high conservation of Lys-197. This finding suggests that the inability to bind calcium

FIGURE 3. **Protealysin regions corresponding to calcium-binding sites of thermolysin (PDB code 8TLN).** *A*, stereoview of Cα backbone superposition of the Ca1/2 region in TLN and the corresponding site in PLN. *B*, stereoview of interaction between analogs of the main Ca^{2+} ligands of Ca1/2 in PLN. *C*, stereoview of Cα backbone superposition of the Ca3 region in TLN and the corresponding site in PLN. *D*, stereoview of Cα backbone superposition of the Ca4 region in TLN and the corresponding site in PLN. *E*, stereoview of PLN region corresponding to the Ca4 site in TLN. TLN is shown in *red*; PLN is shown in *blue*; TLN calcium ions are indicated by *smudged green spheres*; *numbering* corresponds to protealysin; the residues corresponding to the main calcium ligands are shown as *sticks* and labeled by residue name and number; *black numbers* indicate the distance between atoms in angstroms; water molecules are shown as *small red spheres*.

in the region corresponding to Ca1/2 is typical for all protealysin-like TLPs.

The organization of the N-terminal region of mature PLN differs from that of other TLPs with known crystal structures (Fig. 3*C*). This is largely due to a ~30-amino acid shorter N terminus of mature PLN and other M4 enzymes with short propeptides compared with that in TLPs with long propeptides as demonstrated previously by amino acid sequence analysis of TLP precursors (10). The absence of the long sequence underlies a significantly different structure in the region corresponding to calcium-binding site Ca3 of TLN. In addition, PLN residues Asn-79 and Gly-81 correspond to the main ligands interacting with Ca^{2+} by the side chain (Asp-57_{TLN} and Asp-59_{TLN}). Considering that the short N terminus is typical of all protealysin-like enzymes, the absence of the Ca3 site is apparently their common property.

The last calcium-binding site (Ca4) is also significantly different in PLN (Fig. 3, *D* and *E*). First, the PLN molecule has Lys-224 and Ala-218 instead of Asp-200_{TLN} and Thr-194_{TLN}, respectively. Thus, PLN lacks the key ligands of the site, the carboxyl and hydroxyl groups directly interacting with Ca^{2+}. In addition, PLN has a different geometry of the loop forming Ca4 in TLN (Fig. 3*D*), which shifts other calcium ligands: carbonyl oxygens of residues 193_{TLN} (217), 194_{TLN} (218), and 197_{TLN} (221). Such loop conformation in PLN is stabilized by four hydrogen bonds (Lys-224 N–Ala-235 O, Asn-222 O–Asp-237 N, Asn-222 Nδ2–Asp-237 O, and Asn-222 N–Asp-238 Oδ1) with the residues in the structure conserved in protealysin-like proteases (residues 235–244) but missing in TLN. We designated this structure as AYDD-hairpin (Fig. 3*E*) and discussed it below.

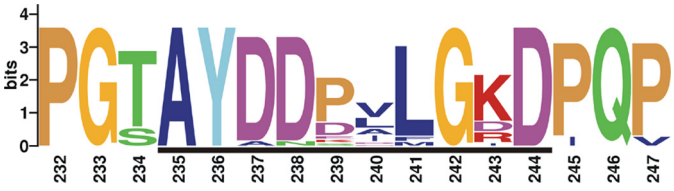

FIGURE 5. **LOGO presentation of consensus sequences of the AYDD-hairpin (*underlined*) and flanking regions of protealysin-like enzymes.** *Numbering* corresponds to proPLN sequence.

This is the first demonstration that an M4 peptidase molecule can lack calcium-binding sites. Note, however, that although proPLN was purified in the presence of calcium ions, no additional calcium salts were added to the precipitant solution during crystallization. Hence, low affinity calcium-binding sites in the PLN molecule cannot be excluded. Their existence is indirectly confirmed by our previous data on decreased PLN thermostability at high Ca^{2+} concentrations (19), which can result from altered structure of the protein after calcium binding by such a low affinity site.

The structure of the PLN catalytic domain differs from known crystal structures of other TLPs not only by the absence of calcium ions. The most significant differences are observed in the active site. All previous three-dimensional structures of M4 peptidases belong to the enzymes with long propeptides. Active sites of these proteins are localized in the cleft between the N- and C-terminal domains (Fig. 4*A*). In PLN, the active site cleft is dammed on the side of the S′ subsites (as designated by Schechter and Berger (40)) (Fig. 4*B*), which provides for extra contacts between the N- and C-terminal domains. The "dam" of the cleft is formed by the above-mentioned AYDD-hairpin (235–244) (Fig. 4C). Our analysis of a representative set of TLP sequences demonstrated that this structural element is absent from known M4 peptidases with long propeptides but present in all enzymes with short propeptides, and its sequence is highly conserved (Fig. 5). Thus, the AYDD-hairpin is a typical feature of protealysin-like enzymes like the short propeptide. Moreover, the propeptide and AYDD-hairpin directly interact, which allows us to consider the AYDD-hairpin as a structural factor providing for the complementarity between the mature portion and propeptide. (The details of the propeptide interaction with the catalytic domain and AYDD-hairpin, in particular, are described below.) In addition, the presence of the AYDD-hairpin changing the active site geometry in the S′ subsites region may be responsible for the narrowed substrate specificity of PLN; we have recently demon-

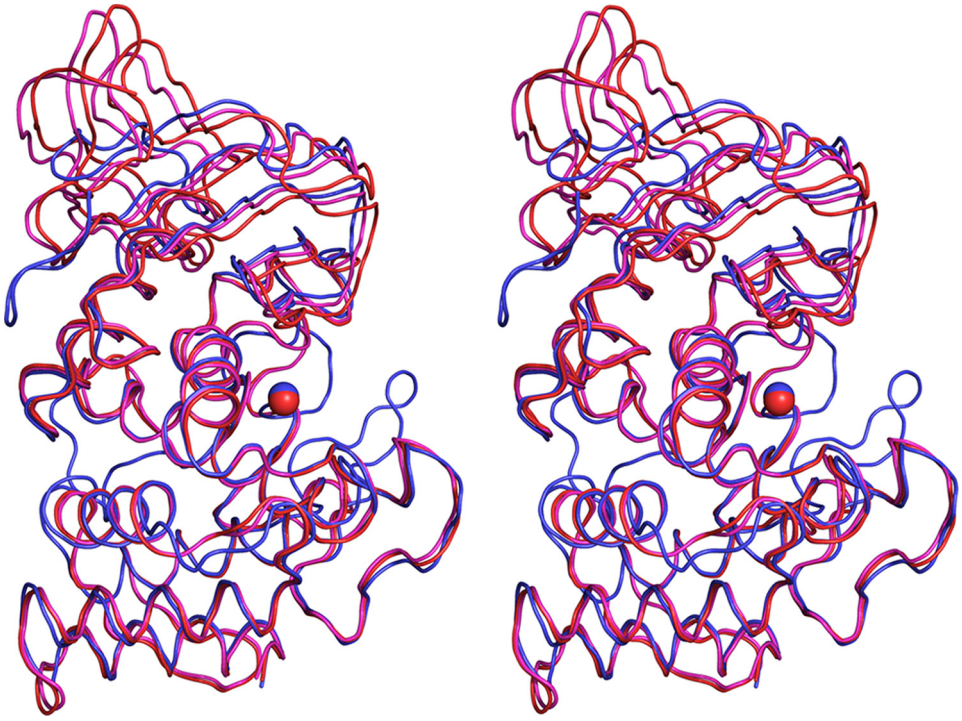

FIGURE 6. **Stereoview of superposition of the Cα backbones in PLN (*blue*) with open (PDB code 1L3F, *magenta*) and closed (PDB code 8TLN, *red*) forms of TLN.** Superposition was made from a three-dimensional alignment of C-terminal domains of the proteins.

strated that, unlike TLN, PLN is highly specific toward actin (41) similar to the homologous protease ECP32/grimelysin (42, 43).

Of note, two crystal forms of TLN and *P. aeruginosa* elastase (PAE) can be produced, depending on whether they bind a ligand or not (8, 44, 45). The enzyme-ligand complexes demonstrate conformations with the "closed" substrate-binding cleft, although free enzymes have more "open" conformations. These data suggested a hinge-bending motion that changes the relative position of the C- and N-terminal domains during the catalytic cycle of TLPs (46). PLN precursor, which can be considered as a mature enzyme in a complex with ligand, has a more open conformation of the substrate-binding cleft than the open form of TLN (Fig. 6) and is nearly as open as the open form of PAE (data not shown). Apparently, this results from the catalytic domain interaction with the propeptide (see below). However, it cannot be excluded that the AYDD-hairpin *per se* prevents approaching of the domains. In this case, mature PLN is incapable of hinge-bending motion during its catalytic cycle and always has an open conformation. Still, this situation is not very probable considering that the open conformation is catalytically unfavorable.

Thus, the PLN catalytic domain has specific properties; it contains no calcium ions and demonstrates substantial differences in the active center region. Our analysis suggests that these changes are not unique to PLN but rather are shared by all TLPs with short propeptides. This allows protealysin-like enzymes to be recognized as an individual subfamily of M4 peptidases based both on the primary structure of their precursors (10) and on the three-dimensional structure of their catalytic domains.

Propeptide Structure and Interaction—As mentioned above, PLN propeptide is an individual domain (Fig. 1) connected to the catalytic domain by a flexible spacer (residues 38–51). Two structural elements can be recognized in the detectable portion of the propeptide (residues 6–37): a hairpin including two α-helices, α1 and α2 (residues 11–22 and 23–36, respectively), and the N-terminal segment (residues 6–10). The propeptide interacts with the catalytic domain in the active site region (Fig. 7, *A* and *B*). The α2 helix contacts the surface of the N-terminal domain of the mature portion; the C-terminal region of α1 contacts the AYDD-hairpin (which can be considered as an element of the C-terminal domain); whereas the N-terminal portion of α1 and the N-terminal segment go down into the socket of the active site.

Helices α1 and α2 contact each other by hydrophobic side chains of Leu-15 and Ile-19 on the α1 side and Arg-27 (aliphatic portion: Cβ, Cγ, and Cδ), Ala-30, Leu-31, and Leu-34 on the α2 side. The α1 and α2 helices interact with the catalytic domain in different ways. Apparently, hydrogen bonds Gln-26 Nϵ2–Glu-148 Oϵ1, Thr-33 Oγ1–Gln-131 N, and Cys-29 Sγ–Glu-129 Oϵ1 are critical in the case of α2. The interactions of α1 are more complex and diverse. The C-terminal portion of α1 realizes a hydrophobic interaction between the side chain of Ile-18 and side chains of Ile-149, Phe-150, Leu-240, and Leu-241 as well as between the aliphatic portion of Arg-17 side chain and Leu-241. Significantly, residues 149 and 150 belong to the N-terminal domain of the PLN mature portion, whereas residues 240 and 241 belong to the AYDD-hairpin, which is a part of the C-terminal domain. Thus, the interaction with the propeptide fixes the N- and C-terminal domains of the proPLN mature portion in a position corresponding to the open conformation of the substrate-binding cleft.

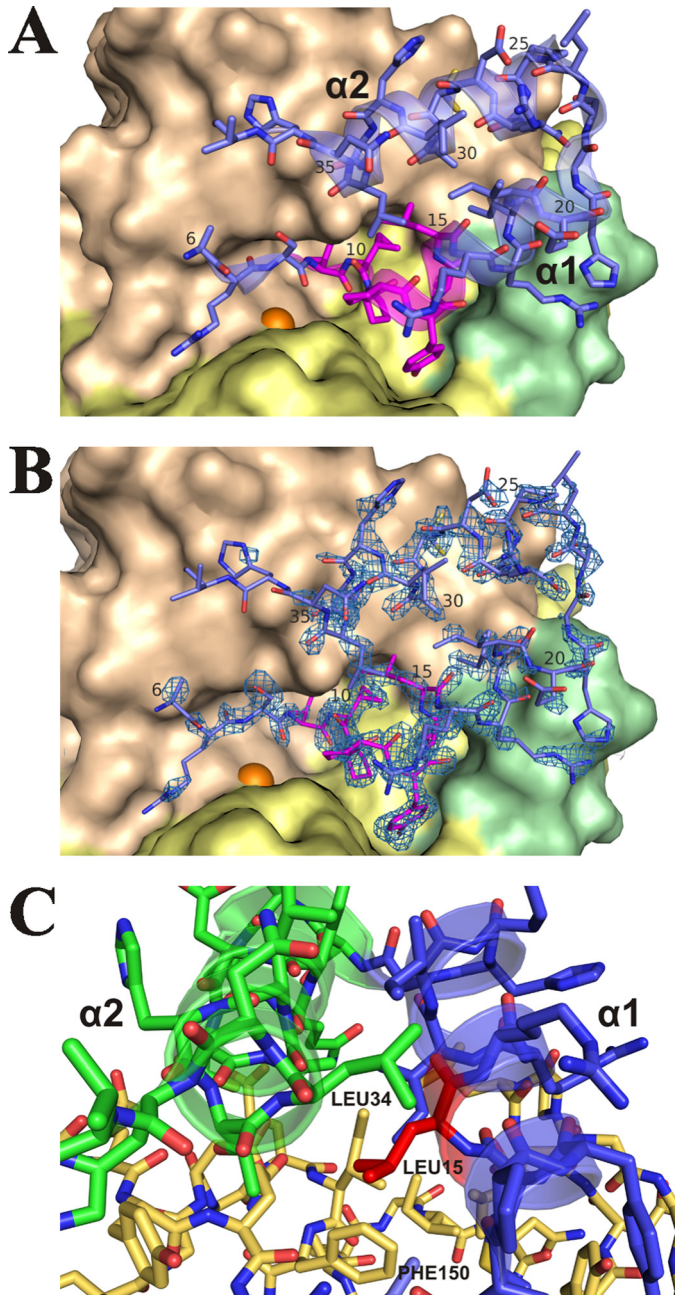

FIGURE 7. **Interaction between protealysin propeptide and catalytic domain.** *A*, general view. *B*, omit map contoured at the 3.0σ level in the propeptide region. In *A* and *B*, mature portion of N-terminal domain is colored *wheat*; C-terminal domain, *yellow*; AYDD-hairpin, *pale green*; the catalytic zinc ion is shown as an *orange sphere*. Propeptide is colored *blue* except for the PPL motif, which is colored *magenta*. *C*, interaction of Leu-15 of the PPL motif. Propeptide: α1 is colored *blue*; α2, *green*; Leu-15, *red*. Mature portion is colored *yellow orange*.

Previously, we have identified a conserved element, the PPL motif, in the short propeptide of TLPs (10). This element is a hydrophobic cluster of seven amino acids, three of which are

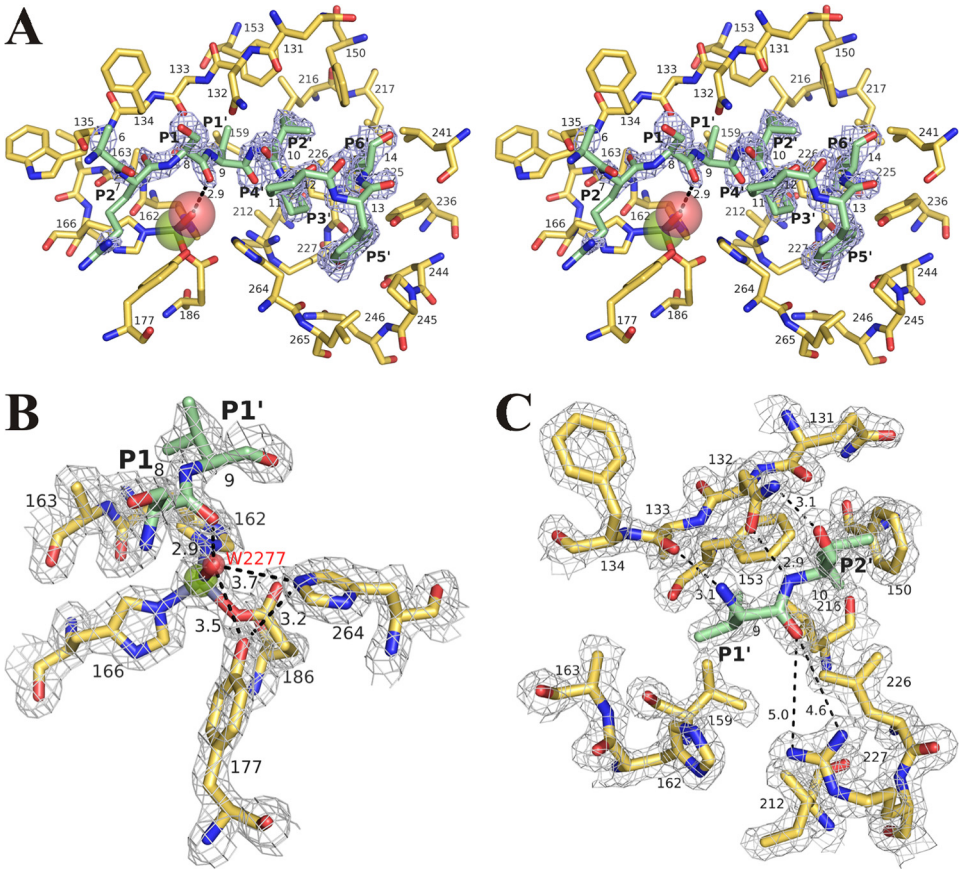

FIGURE 8. **Substrate-binding site of protealysin.** *A*, general stereoview. Omit map contoured at the 3.0σ level in the propeptide region is shown in *light blue*. *B*, environment of the catalytic water molecule. *C*, S1′ and S2′ subsites. In *B* and *C*, electron density map contoured at the 1.5σ level is shown in *light gray*. The catalytic domain is colored *yellow orange*. The propeptide fragments are colored *slate*. Propeptide residues (P1′, P2′) are designated after Schechter and Berger (40). The zinc ion is shown as a *green sphere*; oxygen of HOH-2277, *red sphere*. The distance between atoms is given in angstroms.

In the propeptide-catalytic domain complex, the Ser-8–Val-9 arrangement provides a hydrogen bond distance between the Ser-8 carbonyl group and the water molecule bound by the catalytic zinc (Fig. 8*A*), *i.e.* the Ser-8–Val-9 bond corresponds to the bond hydrolyzed by the active enzyme. (Previously, we have shown that cleavage of this particular bond is the first stage of processing of protealysin precursor (21).) The propeptide residues interacting with the substrate-binding site can be designated as follows in terms of the Schechter and Berger nomenclature (40): Arg-7, P2; Ser-8, P1; Val-9, P1′; Ile-10, P2′; Pro-11, P3′; Pro-12, P4′; Tyr-13, P5′; and Met-14, P6′ (Figs. 2*B* and 8*A*). (Note that P1′-P6′ positions correspond to amino acids in the PPL motif.) Thus, in contrast to all other TLPs with known crystal structures, the S′ region in pro-PLN is substantially extended and formally includes six instead of two subsites (47). The extra subsites are formed due to the AYDD-hairpin conserved in protealysin-like enzymes.

The structure of PLN is the first crystal structure of TLP where the entire S region of the substrate-binding site is occupied by a polypeptide ligand. Previously, peptide interaction with S subsites except S1 were considered only theoretically (47). The data obtained indicate that Ala-6 does not interact with the catalytic domain of the enzyme but is exposed to solvent (Figs. 7*A* and 8*A*). Propeptide residues 2–5, which were undetectable (see above), are likely exposed to solvent too and do not bind to the catalytic domain. This can explain high flexibility of this region. Thus, only the P1 and P2 positions of the peptide ligand nonprimed side are significant for binding to the enzyme. The interaction of the PLN propeptide with the catalytic domain at S2 and S1 is largely analogous to ligand interaction with the substrate-binding site of TLN (47). Arg-7 (P2) and Ser-8 (P1) form an antiparallel β-sheet with the 133–135 region of the catalytic domain. The side chains of residues 7 and 8 point from the active site cleft to solvent (Figs. 7*A* and 8*A*), and their nature is likely not critical for the binding. The crystal structure of proPLN is the first structure of TLP containing an unmodified amino acid at P1 linked to the residue at P1′ with a ordinary peptide bond. Thus, it is the first demonstration of an analog of a substrate-enzyme interaction immediately before the catalytic act. As mentioned above, the carbonyl oxygen of Ser-8 is within hydrogen bond distance from the catalytic water molecule (HOH-2277), which is the fourth ligand of the zinc ion (Fig.

invariant in all protealysin-like enzymes: two neighboring Pro and a Leu two residues downstream of them. An aromatic amino acid Tyr or His immediately follows the Pro-Pro site in most cases. The obtained crystal structure data demonstrate that this motif corresponds to the N-terminal portion of α1 (residues 11–15) and to residues 9 and 10 of the propeptide N-terminal segment (Figs. 2*B* and 7*A*). Six of seven amino acids in the PPL motif directly interact with the S′ substrate-binding subsites of the active site. The last amino acid, Leu-15, residing between α1, α2, and the N-terminal domain of the mature portion is likely one of the main bridging elements that stabilizes the propeptide-catalytic domain complex (Fig. 7*C*). Phe-150 in the mature portion and Leu-34 in α2 are the main partners of Leu-15.

The N-terminal region of the propeptide (residues 7–14) occupies the substrate-binding site of PLN (Fig. 8*A*). Hence, the interaction between the catalytic domain and this propeptide region can be considered analogous to the interaction between the enzyme and substrate (and the propeptide is essentially the substrate (21)). Note the peculiar structure of the propeptide: it has a specific sequence and is anchored by the α-helical hairpin. In this context, one cannot exclude that the peptide substrate binding to the active site of PLN in general can differ from the propeptide binding.

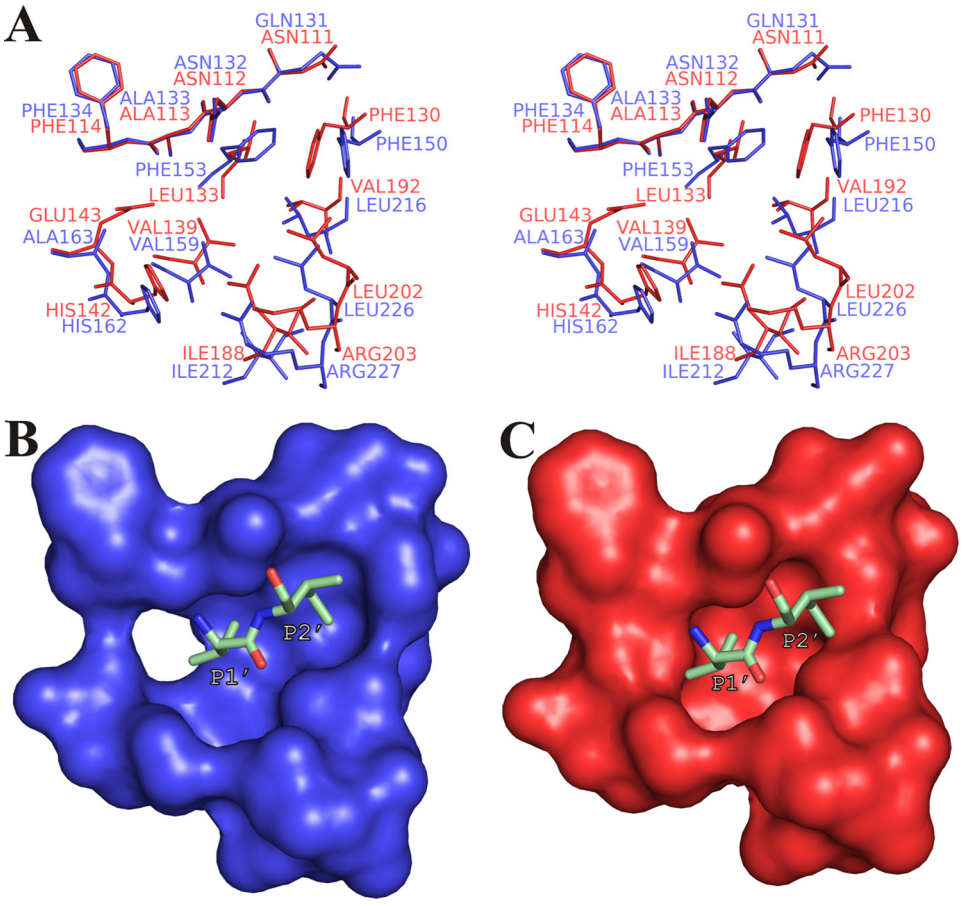

FIGURE 9. **Comparison of the S1′, S2′ pocket of protealysin and S1′ pocket of thermolysin (PDB code 8TLN).** *A*, stereoview of superposed residues forming the S1′ and S2′ sites of PLN (*blue*) and TLN (*red*). *B*, S1′, S2′ pocket of PLN. Residue positions correspond to *A*. *C*, S1′ pocket of TLN. Residue positions correspond to *A*. Val-9 and Ile-10 of proPLN are shown as *sticks* in *B* and *C* and are designated after Schechter and Berger (40).

8*B*). The phenol group of Tyr-177 (157_{TLN}) and the Nϵ2 nitrogen atom of the imidazole ring of His-264 (231_{TLN}), which are the residues stabilizing an intermediate state of the substrate similar to the "oxyanion hole" of serine proteases (48), are oriented toward HOH-2277. The Tyr-177 OH–HOH-2277 O and His-264 Nϵ2–HOH-2277 O distances in the structure of proPLN are greater than the length of a strong hydrogen bond. Still, such bonds cannot be excluded in a mature molecule bond to the substrate and with a closed conformation of the substrate-binding cleft. At the same time, the Tyr-177 OH–His-264 Nϵ2 bond is likely formed in the proPLN molecule.

The PLN propeptide interaction with the catalytic domain at the S1′ and S2′ regions is similar to the ligand interaction with the analogous sites in TLN (47) and PAE (44). The main chain of the propeptide at the Val-9 (P1′)–Ile-10 (P2′) region forms three hydrogen bonds with the Asn-132-Ala-133 region of the catalytic domain: Val-9 N–Ala-133 O, Ile-10 N–Asn-132 Oδ1, and Ile-10 O–Asn-132 Nδ2 (Fig. 8*C*). At the same time, the Val-9 O–Arg-227 NH1 and Val-9 O–Arg-227 NH2 distances are much longer than the hydrogen bond length, whereas hydrogen bonds between the carbonyl residue at the P1′ position and the corresponding groups of $Arg\text{-}203_{TLN}$ (198_{PAE}) are formed after ligand interaction with TLN and PAE. This situation similar to the above-mentioned interaction of Tyr-177 and His-264 with HOH-2277 can result from the open conformation of the proPLN substrate-binding cleft. We believe that hydrogen bonds between Val-9 and Arg-227 are formed during ligand binding by the mature enzyme.

The S1′ site is the major determinant of substrate specificity in TLPs (49, 50). Similar to other M4 peptidases, PLN has a hydrophobic pocket in the binding region of the side chains of the amino acid at position P1′, which, however, notably differs from the S1′ pocket of TLN (Fig. 9). Phe-153, Val-159, Leu-216, and Leu-226 (corresponding to $Leu\text{-}133_{TLN}$, $Val\text{-}139_{TLN}$, $Val\text{-}192_{TLN}$, and $Leu\text{-}202_{TLN}$, which form the S1′ pocket of TLN) contribute most to the region formation in PLN (Fig. 9*A*). At the same time, bulkier amino acids (Phe-153 *versus* $Leu\text{-}133_{TLN}$ and Leu-216 *versus* $Val\text{-}192_{TLN}$) make the S1′ pocket of PLN shallower compared with that of TLN. Presumably, PLN has a higher hydrolytic preference toward bonds formed by α-amino groups of small hydrophobic residues such as Ala or Val than TLN and other TLPs with a TLN-like structure of the S1′ pocket. The presence of a pronounced S2′ pocket is an important feature of the proPLN structure (Fig. 9*B*); this pocket results from the shift of Phe-150 ($Phe\text{-}130_{TLN}$) and "elongation" of the S1′ pocket relative to TLN (Fig. 9*C*). Thus, the efficiency of substrate binding should depend on the amino acid at the position of the P2′ substrate more for PLN than for TLN.

As mentioned above, the S′ region in TLN and other TLPs with previously known three-dimensional structures contains only two subsites (47), whereas the catalytic domain of proPLN contains additional S′ subsites interacting with residues 11–14 of the propeptide (Fig. 10*A*). Because this is the most conserved region in the short propeptides, its contacts are likely crucial for their functioning. Pro-11 and Pro-12 corresponding to ligand positions P3′ and P4′ are conserved in all short propeptides without exception and, likely, provide for a precise steric complementarity between the propeptide and the catalytic domain; a tandem of prolines lowers the polypeptide chain at the N terminus of the α1 helix. Well defined binding pockets in the mature portion correspond to the side chains of Tyr-13 (P5′) and Met-14 (P6′) (Fig. 10*A*). The S5′ pocket is a large cavity, whose entrance is formed by hydrophobic side chains of Pro-245 and Leu-265 contacting the aromatic ring of Tyr-13

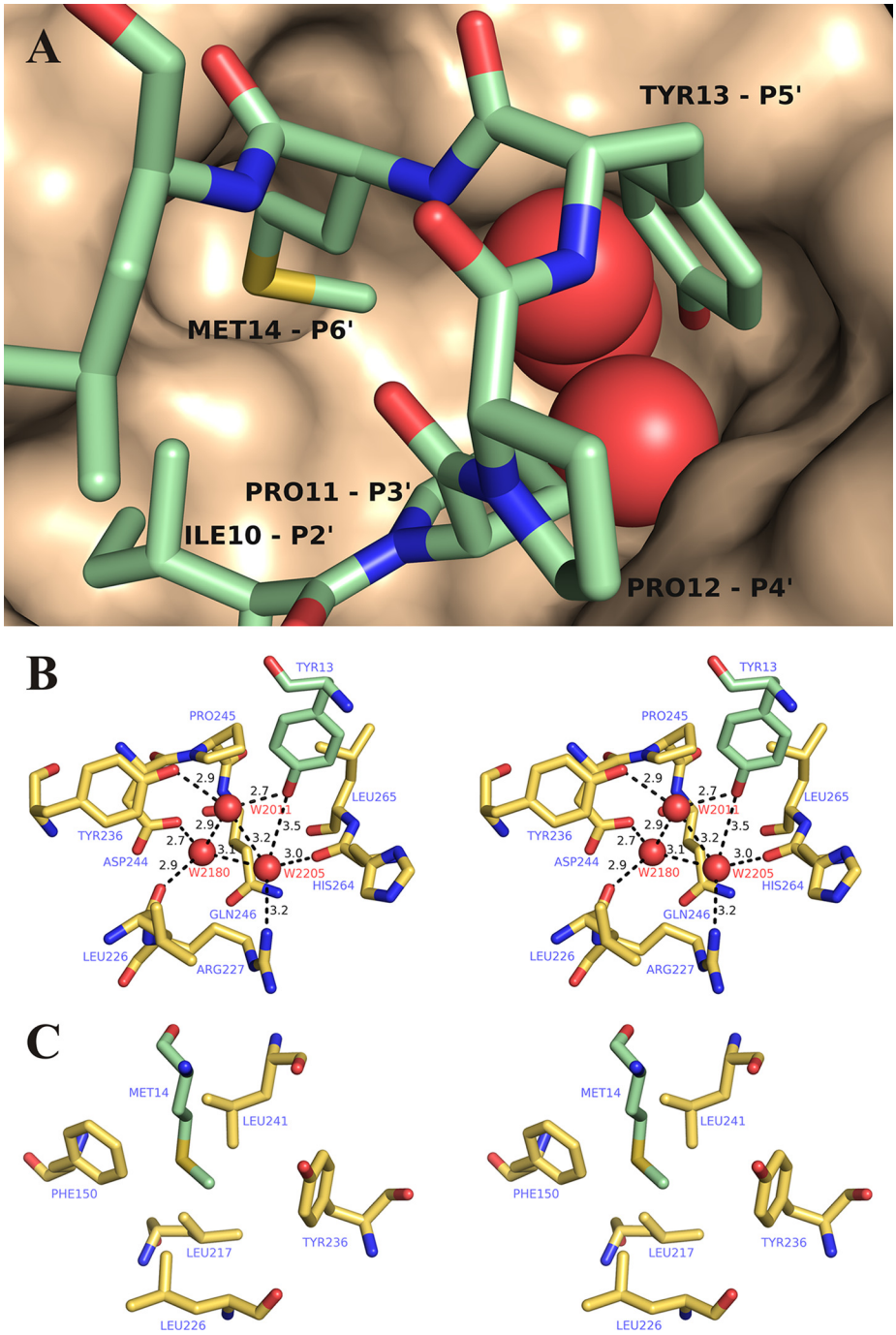

FIGURE 10. **S3′-S6′ subsites of protealysin.** *A*, general view. The catalytic domain surface is shown. Propeptide residues (P2′-P6′) are designated after Schechter and Berger (40). *B*, S5′ pocket. *C*, S6′ pocket. Mature portion residues is colored *yellow orange*. Propeptide residues are colored *pale green*. Oxygen molecules of HOH-2011, HOH-2180, and HOH-2205 are shown as *red spheres*. The distance between atoms is given in angstroms.

(Fig. 10*B*). Deep in the pocket, there is a cluster of three water molecules (HOH-2011, HOH-2180, and HOH-2205) linked to the residues of the catalytic domain (Leu-226, Arg-227, Tyr-236, Asp-244, and His-264) and to each other with a network of hydrogen bonds. (Note that each water molecule in this cluster forms the highest possible number of hydrogen bonds.) The phenol hydroxyl group of Tyr-13 is also involved in this network with a hydrogen bond with water molecule HOH-2011.

This organization of the S5′ pocket makes it clear why a pair of prolines in the short propeptides of TLPs is usually followed by an aromatic residue, Tyr or His, capable of forming hydrogen bonds. The S6′ pocket has a much simpler structure of a hydrophobic hollow formed by Phe-150, Leu-226, Tyr-236, Leu-241, and Leu-217 (Fig. 10*B*). The first four residues likely contribute most to the interaction with Met-14. It should be stressed that, because the conserved residues of the AYDD-hairpin are crucial for the S5′ and S6′ subsites formation (Fig. 5), the observed structure is most likely not unique to the discussed molecule but rather is shared by all protealysin-like proteins.

Analysis of all interactions between the prosequence and the catalytic domain suggests that propeptide of PLN is an intramolecular inhibitor. The inhibitory effect of the prosequence most likely involves blocking the S′ substrate-binding region of the enzyme by the propeptide region corresponding to the PPL motif and the fixation of the catalytically unfavorable open conformation of the active site.

CONCLUSIONS

Analysis of the proPLN crystal structure, which is the first structure of M4 peptidase precursor, suggests that protealysin-like proteases can be considered as an individual subfamily of TLPs on the basis of both precursor and catalytic domain structure. Typical features of the catalytic domain of PLN and likely other M4 peptidases with short propeptides include the absence of calcium-binding sites, different N-terminal structure, and presence of the highly conserved AYDD-hairpin modifying the structure of the substrate-binding region.

The propeptide of PLN forms a separate domain of the protein and likely acts as an intramolecular inhibitor blocking the substrate-binding region and fixing the catalytically unfavorable open conformation of the enzyme active site. The key elements of the propeptide-mature portion interface in proPLN include the AYDD-hairpin in the catalytic domain and the highly conserved PPL motif in the propeptide.

REFERENCES

1. Rawlings, N. D., and Barrett, A. J. (1995) *Methods Enzymol.* **248,** 183–228
2. Rawlings, N. D., Morton, F. R., Kok, C. Y., Kong, J., and Barrett, A. J. (2008) *Nucleic Acids Res.* **36,** D320–325
3. Adekoya, O. A., and Sylte, I. (2009) *Chem. Biol. Drug. Des.* **73,** 7–16
4. Titani, K., Hermodson, M. A., Ericsson, L. H., Walsh, K. A., and Neurath, H. (1972) *Biochemistry* **11,** 2427–2435
5. Matthews, B. W., Jansonius, J. N., Colman, P. M., Schoenborn, B. P., and Dupourque, D. (1972) *Nature New. Biol.* **238,** 37–41
6. Pauptit, R. A., Karlsson, R., Picot, D., Jenkins, J. A., Niklaus-Reimer, A. S., and Jansonius, J. N. (1988) *J. Mol. Biol.* **199,** 525–537
7. Stark, W., Pauptit, R. A., Wilson, K. S., and Jansonius, J. N. (1992) *Eur. J. Biochem.* **207,** 781–791
8. Thayer, M. M., Flaherty, K. M., and McKay, D. B. (1991) *J. Biol. Chem.* **266,** 2864–2871
9. Banbula, A., Potempa, J., Travis, J., Fernandez-Catalán, C., Mann, K., Huber, R., Bode, W., and Medrano, F. (1998) *Structure* **6,** 1185–1193
10. Demidyuk, I. V., Gasanov, E. V., Safina, D. R., and Kostrov, S. V. (2008) *Protein J.* **27,** 343–354
11. McIver, K. S., Kessler, E., Olson, J. C., and Ohman, D. E. (1995) *Mol. Microbiol.* **18,** 877–889
12. Braun, P., Tommassen, J., and Filloux, A. (1996) *Mol. Microbiol.* **19,** 297–306
13. Marie-Claire, C., Ruffet, E., Beaumont, A., and Roques, B. P. (1999) *J. Mol. Biol.* **285,** 1911–1915
14. Tang, B., Nirasawa, S., Kitaoka, M., Marie-Claire, C., and Hayashi, K. (2003) *Biochem. Biophys. Res. Commun.* **301,** 1093–1098
15. Kessler, E., and Safrin, M. (1994) *J. Biol. Chem.* **269,** 22726–22731
16. O'Donohue, M. J., and Beaumont, A. (1996) *J. Biol. Chem.* **271,** 26477–25481
17. Serkina, A. V., Gorozhankina, T. F., Shevelev, A. B., and Chestukhina, G. G. (1999) *FEBS Lett.* **456,** 215–219
18. Wetmore, D. R., Wong, S. L., and Roche, R. S. (1992) *Mol. Microbiol.* **6,** 1593–1604
19. Demidyuk, I. V., Kalashnikov, A. E., Gromova, T. Y., Gasanov, E. V., Safina, D. R., Zabolotskaya, M. V., Rudenskaya, G. N., and Kostrov, S. V. (2006) *Protein. Expr. Purif.* **47,** 551–561
20. Gromova, T., Demidyuk, I., Kostrov, S., Sosfenov, N., Melik-Adamyan, V., and Kuranova, I. (2008) *Crystallogr. Rep.* **53,** 793–795
21. Gromova, T. Y., Demidyuk, I. V., Kozlovskiy, V. I., Kuranova, I. P., and Kostrov, S. V. (2009) *Biochimie* **91,** 639–645
22. Dodonov, A. F., Loboda, A. V., Kozlovski, V. I., Soulimenkov, I. V., Raznikov, V. V., Zhen, Z., Horwath, T., and Wollnik, H. (2000) *Eur. J. Mass Spectro.* **6,** 481–490
23. Kheiker, D., Kovalchuk, M., Shilin, Y., Shishkov, V., Sulyanov, S., Dorovatovskii, P., and Rusakov, A. (2007) *Crystallogr. Rep.* **52,** 358–364
24. Kabsch, W. (1993) *J. Appl. Crystallogr.* **26,** 795–800
25. Long, F., Vagin, A. A., Young, P., and Murshudov, G. N. (2008) *Acta Crystallogr. D Biol. Crystallogr.* **64,** 125–132
26. Vagin, A., and Teplyakov, A. (1997) *J. Appl. Crystallogr.* **30,** 1022–1025
27. (1994) *Acta Crystallogr. D Biol. Crystallogr.* **50,** 760–763
28. Murshudov, G. N., Vagin, A. A., and Dodson, E. J. (1997) *Acta Crystallogr. D Biol. Crystallogr.* **53,** 240–255
29. Emsley, P., and Cowtan, K. (2004) *Acta Crystallogr. D Biol. Crystallogr.* **60,** 2126–2132
30. Read, R. J. (1986) *Acta Crystallogr. Sect. A* **42,** 140–149
31. Thompson, J. D., Gibson, T. J., Plewniak, F., Jeanmougin, F., and Higgins, D. G. (1997) *Nucleic Acids Res.* **25,** 4876–4882
32. Schneider, T. D., and Stephens, R. M. (1990) *Nucleic Acids Res.* **18,** 6097–6100
33. Crooks, G. E., Hon, G., Chandonia, J. M., and Brenner, S. E. (2004) *Genome Res.* **14,** 1188–1190
34. Guex, N., and Peitsch, M. C. (1997) *Electrophoresis* **18,** 2714–2723
35. DeLano, W. L. (2007) *The PyMOL Molecular Graphics System*, DeLano Scientific LLC, San Carlos, CA
36. Dahlquist, F. W., Long, J. W., and Bigbee, W. L. (1976) *Biochemistry* **15,** 1103–1111
37. Roche, R. S., and Voordouw, G. (1978) *CRC Crit. Rev. Biochem.* **5,** 1–23
38. Corbett, R. J., and Roche, R. S. (1983) *Biopolymers* **22,** 101–105
39. Veltman, O. R., Vriend, G., Berendsen, H. J., Van den Burg, B., Venema, G., and Eijsink, V. G. (1998) *Biochemistry* **37,** 5312–5319
40. Schechter, I., and Berger, A. (1967) *Biochem. Biophys. Res. Commun.* **27,** 157–162
41. Tsaplina, O. A., Efremova, T. N., Kever, L. V., Komissarchik, Y. Y., Demidyuk, I. V., Kostrov, S. V., and Khaitlina, S. Y. (2009) *Biochemistry* **74,** 648–654
42. Khaitlina, SYu, Smirnova, T. D., and Usmanova, A. M. (1988) *FEBS Lett.* **228,** 172–174
43. Bozhokina, E., Khaitlina, S., and Adam, T. (2008) *Biochem. Biophys. Res. Commun.* **367,** 888–892
44. McKay, D. B., Thayer, M. M., Flaherty, K. M., Pley, H., and Benvegnu, D. (1992) *Matrix Suppl.* **1,** 112–115
45. Hausrath, A. C., and Matthews, B. W. (2002) *Acta Crystallogr. D Biol. Crystallogr.* **58,** 1002–1007
46. Holland, D. R., Tronrud, D. E., Pley, H. W., Flaherty, K. M., Stark, W., Jansonius, J. N., McKay, D. B., and Matthews, B. W. (1992) *Biochemistry* **31,** 11310–11316
47. Hangauer, D. G., Monzingo, A. F., and Matthews, B. W. (1984) *Biochemistry* **23,** 5730–5741
48. Matthews, B. W. (1988) *Acc. Chem. Res.* **21,** 333–340
49. Feder, J. (1967) *Biochemistry* **6,** 2088–2093
50. Feder, J., and Schuck, J. M. (1970) *Biochemistry* **9,** 2784–2791
51. Diederichs, K., and Karplus, P. A. (1997) *Nat. Struct. Biol.* **4,** 269–275
52. Davis, I. W., Leaver-Fay, A., Chen, V. B., Block, J. N., Kapral, G. J., Wang, X., Murray, L. W., Arendall, W. B., 3rd, Snoeyink, J., Richardson, J. S., and Richardson, D. C. (2007) *Nucleic Acids Res.* **35,** W375–383